Pis'ma v ZhETF, vol. 96, iss. 5, pp. 347 – 351

Structure of π- and 2π-walls in smectic films

P. V. Dolganov, V. K. Dolganov, P. Cluzeau[+]

Institute of Solid State Physics of the RAS, 142432 Chernogolovka, Russia

[+]*Université Bordeaux I, CNRS, Centre de Recherche Paul Pascal, Avenue A. Schweitzer, 33600 Pessac, France*

Submitted 23 July 2012

The structure of π- and 2π-walls in smectic films was reconstructed from optical reflectivity measurements. Investigations were made in free standing films of nonpolar Smectic-C and ferroelectric Smectic-C^* liquid crystals. π-walls are observed in magnetic field and 2π-walls in electric field parallel to the film plane. For the first time the distribution of molecular orientation across the walls was determined. Peculiarities of the wall structure related to the anisotropy of the film elasticity were found. The structure of the walls is well described by the theory taking into account the anisotropy of two-dimensional elasticity of smectic films.

In external magnetic or electric field π-walls and 2π-walls are typical soliton-type orientational defects in liquid crystals [1, 2]. They separate regions with liquid crystal orientation energetically equivalent with respect to external field. Depending on the mechanism of interaction of external field with the liquid crystal, π- or 2π-walls can be formed. Investigation of the walls is important both for fundamental physics and applications [2–6]. Wall structure and dynamics are governed by fundamental characteristics of liquid crystals, namely, elasticity and viscosity. Wall nucleation and motion result in the reorientation of the molecules and play an important role in different electro- and magneto-optical effects.

In spite of numerous observations of walls in smectic films [4–9], up to now orientation of the liquid crystal across the walls was not experimentally determined. The wall structure was characterized as a rule only by relative positions of dark and bright stripes which are observed in crossed polarizers. These stripes correspond to several selected molecular orientations, which do not reflect all the peculiarities of the wall structure. In our studies we analyzed the structure of π-walls and 2π-walls in detail. For the first time the continuous distribution of liquid crystal orientation across the walls was measured. The peculiarities of the wall structure are related to the two-dimensional ($2D$) elasticity and essentially depend on the wall orientation with respect to the field direction. Our measurements allow us to perform a quantitative comparison of the wall structure with theory.

In this paper, the walls are studied in nonpolar Smectic-C (SmC) and ferroelectric Smectic-C^* (SmC^*) liquid crystals. Our investigations were made in free standing films [10]. In these films the smectic layers are parallel to the free surfaces. In SmC and SmC^* the long molecular axes tilt by an angle θ with respect to the layer normal (Fig. 1a and b). Projections of the long molecular axes onto the layer plane form the $2D$ field of molecular ordering or the so-called **c**-director field. In the ferroelectric phase the layers possess spontaneous polarization $\boldsymbol{P}$ which orients perpendicular to the tilt plane and to the **c**-director.

The experiments were carried out on racemic 4'-undecyloxybiphenys-4-yl 4-(1-metthylheptyloxy)benzoate (11BSMHOB) [11, 12] and on a mixture of racemic 11BSMHOB and chiral 11BSMHOB isomer (9.6 %). The mixture exhibits the ferroelectric SmC^* instead of the SmC phase in racemic 11BSMHOB. The sequence of phase transitions in the bulk sample was SmC^*–(108.3 °C)–Cholesteric–(123.9 °C)–Isotropic in the chiral material and SmC–(108.3 °C)–Nematic–(124 °C)–Isotropic in the racemate. Polarization P of the employed mixture was evaluated from the relation $P = P_0 X$ [13], where $P_0 = 40\,\mathrm{nC/cm^2}$ is the polarization of the chiral isomer and X is the concentration of the isomer in the mixture with racemate. The tilt angle in 11BSMHOB is close to 45° and is practically temperature independent [11]. Polarization of ferroelectric is also practically temperature independent. In SmC films π-walls were observed in magnetic field parallel to the film plane. Films were prepared by drawing a small amount of the material in the smectic phase across a 4-mm hole in a glass plate. The glass plate with the film was placed in a thermostatic cell between two permanent magnets (Fig. 1c). 2π-walls were observed in ferroelectric SmC^* films in an electric field. Ferroelectric films were prepared in a rectangular hole (10×1 mm^2). The electric field was applied between two metallic blades. Investigations were made on films with thickness N of 5–8 molecular layers, which was much less than the helical pitch of the ferroelectric phase. Thin free-standing films do not melt

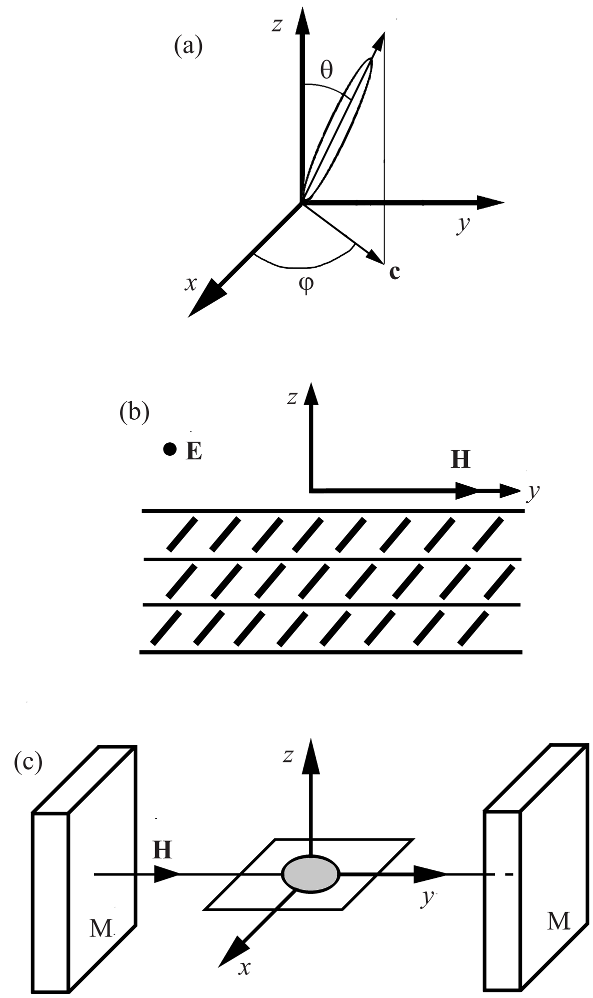

Fig. 1. Schematic representation of the molecule in a tilted smectic phase (a), smectic film with layer structure and orientation of electric and magnetic field (b), experimental geometry for the measurements in magnetic field (c). The smectic film for magnetic measurements was prepared in a circular hole in a rectangular glass plate

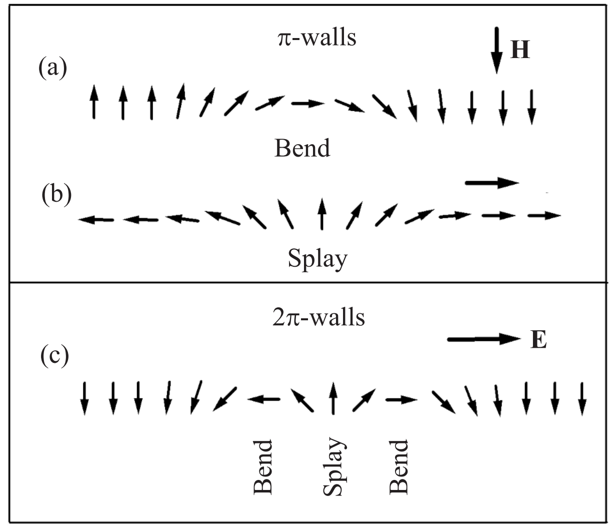

Fig. 2. Schematic representation of the **c**-director orientation in π-walls in magnetic field (a), (b) and 2π-walls in electric field (c). The orientation of magnetic (**H**) and electric (**E**) field is shown above every wall. Regions with mainly bend and splay deformation are shown in π- and 2π-walls

on heating but undergo thinning transitions [14]. The investigated films can exist at the temperature 10 °C above the bulk SmC^*-Cholesteric (or SmC-Nematic) transition. Film thickness was determined by optical reflectivity measurements [15]. Reflected light intensity across the walls was measured using a CCD camera with calibrated sensitivity curve.

In nonpolar SmC, the **c**-director was oriented by external magnetic field **H** directed in the film plane. The orientations of the **c**-director parallel or antiparallel to **H** correspond to the minimum of magnetic energy $-\chi_a H^2/2\sin^2\theta$, where χ_a is the magnetic anisotropy [1]. So, walls in the film can separate regions with opposite **c**-director orientations and are thus π-walls (Fig. 2a and b). In ferroelectric SmC^*, the **c**-director can be oriented by the interaction of the electric field **E** with layer polarization. The minimum of electrostatic energy $-\mathbf{PE}$ corresponds to the orientation of polarization **P** parallel to **E**. So, 2π-walls are formed in polar films and separate regions with parallel **c**-director orientation (Fig. 2c). A schematic representation of the **c**-director orientation across the π- and 2π-walls is shown in Fig. 2. The measurements of the structure of π-walls were made both for the walls oriented parallel and perpendicular to the magnetic field (Fig. 2a and b). The 2π-walls oriented perpendicular to the metallic blades are not rigidly attached to the blades by their ends. They can move slowly parallel to the blades. Motion of the 2π-walls oriented parallel to the electric field does not allow performing precise measurements of their structure. Investigations were made on 2π-walls oriented perpendicular to the electric field (Fig. 2c).

In this paper the director orientation was determined in polarized light reflectivity experiments. The incident light polarization was parallel to the **c**-director orientation far from the walls. The intensity reflected from the film depends on the orientation of the **c**-director relative to the direction of incident light polarization. Curves *a* and *b* in Fig. 3 show the measured reflected light intensity across the π-walls oriented parallel (the solid curve) and perpendicular (the dashed curve) to the magnetic field. The intensity was normalized by the reflected light far from the walls $I_{||}$. As one can see from Fig. 3, in

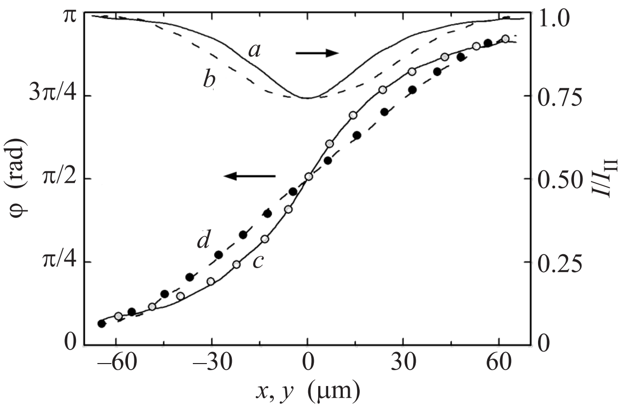

Fig. 3. The reflected light intensity (bands a and b) across the π-walls in magnetic field. The polarization of incident light was parallel to the **c**-director far from the walls. Two bands a and b represent the relative light intensity $I/I_{||}$ for walls oriented parallel (solid curve) and perpendicular (dashed curve) to the far-field **c**-director. $I_{||}$ is the intensity of the light with polarization parallel to the far-field **c**-director. Solid and dashed S-shaped curves (c, d) show the angle of the **c**-director orientation φ across the walls deduced from the reflected intensities (bands a and b) using Eq. (2). Solid and open points are the results of the numerical calculations of φ using Eq. (4) and values $\chi_a H^2/K_B = 5.2 \cdot 10^5$ cm^{-2}, $\chi_a H^2/K_S = 1.42 \cdot 10^5$ cm^{-2}; $H = 3 \cdot 10^3$ Oe, racemic 11BSMHOB mixture; $N = 8$, $T = 104\,^\circ$C

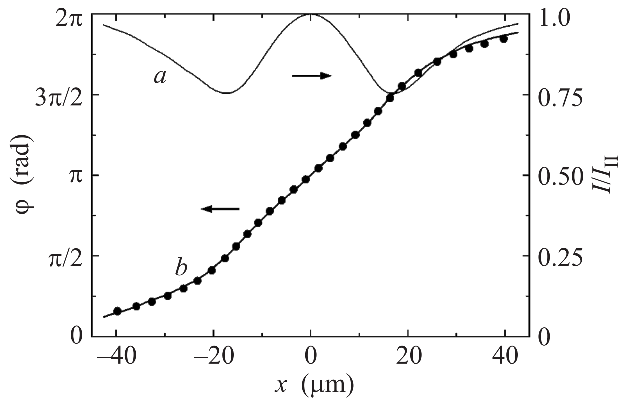

Fig. 4. The upper curve with two minima (a) represents the relative light intensity $I/I_{||}$ measured across the 2π-wall oriented parallel to the far-field **c**-director. Polarization of incident light was parallel to the **c**-director far from the walls. The S-shaped curve (b) is the angle of the **c**-director rotation deduced from the experimental data. Solid points are the results of the numerical calculations of φ using Eq. (5) and values $PE/K_S = 1.65 \cdot 10^5\,\mathrm{cm}^{-2}$ and $PE/K_B = 4.95 \cdot 10^5\,\mathrm{cm}^{-2}$. Chiral 11BSMHOB, $X = 9.6\%$, $E = 11.5$ V/cm, $N = 6$, $T = 103\,^\circ$C

reflected light the π-wall looks like a darker stripe on bright background. The intensity of the reflected light is maximal $I_{||}$ far from the walls when the orientation of the **c**-director coincides with polarization of the incident light and is minimal $I_\perp$ when the **c**-director is perpendicular to the polarization of the incident light, i.e. in the center of the π-walls. The band widths essentially differ for two orientations of the walls. Fig. 4 (curve a) shows the reflected intensity across the 2π-wall for light polarization perpendicular to the electric field. In this geometry, 2π-walls look like two darker stripes on bright background.

The intensity of light reflected from the film I depends on the angle φ between the **c**-director and the polarization of incident light, that is, on the angle of the **c**-director orientation with respect to its orientation far from the wall. The intensity also depends on the reflectivity of the light polarized along the **c**-director $I_{||}$ and perpendicular to it $I_\perp$. For thin films employed in the experiment I may be written [15] as

$$I(\varphi) = I_{||} \cos^2 \varphi + I_\perp \sin^2 \varphi. \tag{1}$$

Eq. (1) allows us to determine φ and thus the orientation of the **c**-director across the wall from the intensity of the reflected light:

$$\varphi = \arccos \sqrt{[I(\varphi) - I_\perp] / \left(I_{||} - I_\perp\right)}. \tag{2}$$

The solid (c) and dashed (d) curves in Fig. 3 represent the orientation of the **c**-director across the π-walls deduced from the reflectivity (bands a and b) using Eq. (2). The director orientation across the 2π-wall determined from the reflectivity is shown by the lower solid curve in Fig. 4.

The structure of the walls depends on the $2D$ orientational splay and bend elastic constants K_S and K_B [1]. The detailed structure of the walls obtained in our experiment enables to make comparison with theory and to determine both elastic constants. In the one-constant approximation ($K_B = K_S = K$) the 2π-wall structure $\varphi(x)$ in electric field is described by a transcendental equation $\tan \varphi/4 = \pm \exp\left(-|x|/\xi\right)$, where the correlation length $\xi = (K/PE)^{1/2}$ [4]. The largest slope $d\varphi/dx$ in the walls should be located in their center (namely, for $\varphi = \pi$). This does not correspond to experiment (Fig. 4). The largest slopes are shifted from the wall center towards the points where $\varphi = \pi/2$ and $\varphi = 3\pi/2$. The peculiarity of the wall structure is determined by the change of the contribution of the bend and splay deformation across the wall and the anisotropy of the elasticity. In the regions of the 2π-wall near $\varphi = \pi/2$ and

$3\pi/2$ the elastic deformation is mostly bend, whereas in the wall center the deformation is splay (Fig. 2c). The largest slope in the 2π-wall observed not in the wall center should be related with large elastic anisotropy of the **c**-director field ($K_S > K_B$). In the π-walls the largest slope is in the wall center. This is best obvious for the π-wall parallel to the magnetic field (Fig. 3, curve c). In the one-constant approximation ($K_S = K_B$) the wall structure does not depend on the wall orientation with respect to the field. This is not the case in Fig. 3. The distribution of the **c**-director orientation in the wall essentially differs for two wall orientations. The observed difference in the wall structure (Fig. 3) is explained by the anisotropy of the elasticity ($K_S > K_B$). In the center of the π-wall the deformation of the **c**-director is pure bend for the wall parallel to the field and pure splay for the wall perpendicular to it (Fig. 2a and b).

The elastic theory of the **c**-director field [1] can be used to calculate the structure of the walls. To describe the **c**-director orientation in the walls, we consider the free energy of the tilted smectic per film thickness in the external field [1]:

$$F = \int \left[\frac{1}{2}K_S\left(\nabla\cdot\mathbf{c}\right)^2 + \frac{1}{2}K_B\left(\nabla\times\mathbf{c}\right)^2 + F_{in}\right] dxdy. \quad (3)$$

The first two terms give the standard elastic free energy. The third term describes the interaction of the liquid crystal with external field. For a nonpolar SmC film the interaction with magnetic field is $F_{in} = -\chi_a\left(\mathbf{c}\cdot\mathbf{H}\right)^2/2\sin^2\theta$, for a ferroelectric Sm$C^*$ film the interaction with electric field is $F_{in} = -\left(\mathbf{P}\cdot\mathbf{E}\right)$. In our experiments we used small values of the electric field. Using the results of Ref. [16] in which the transition from 2π-walls to π-walls was observed due to dielectric anisotropy term [1], we obtain that in order for the dielectric term to be essential the electric field in our measurements should be 10^3 times larger than the one we used. So in our case the dielectric term is not used. Another question may arise about the influence of polarization space charge [13, 17]. Influence of polarization space charge on wall structure can be essential for samples with high polarization. Space charge can lead to renormalization of the elastic constants [13, 17]. In our case the ratio of elastic constants (measurement accuracy of about ±10 percent) in the racemate and in SmC^* practically does not change. It shows that the influence of polarization charges is not essential.

In Eq. (3) the **c**-director has a fixed length $|\mathbf{c}| = 1$ but can change its orientation. Minimizing the free energy (3) with respect to the distribution of the **c**-director orientation across the wall, we find for the film in magnetic field:

$$\varphi'_{x,y} = \left[\frac{\chi_a H^2\sin^2\theta\sin^2\varphi}{K_\varphi}\right]^{1/2}. \quad (4)$$

In Eq. (4) $K_\varphi = K_S\sin^2\varphi + K_B\cos^2\varphi$ and $\varphi' = d\varphi/dx$ for the wall parallel to the field, $K_\varphi = K_S\cos^2\varphi + K_B\sin^2\varphi$ and $\varphi' = d\varphi/dy$ for the wall perpendicular to the field [8]. Minimizing F for the case of the electric field yields:

$$\varphi'_x = \left[\frac{2PE\left(1-\cos\varphi\right)}{K_\varphi}\right]^{1/2}, \quad (5)$$

where $K_\varphi = K_B\cos^2\varphi + K_S\sin^2\varphi$ for the wall perpendicular to the field. Eqs. (4) and (5) have the uniform solution $\varphi = \mathrm{const}$ and the soliton solutions. We will consider the soliton solutions with a single soliton (a π-wall or a 2π-wall). Comparing the measured distances in π-walls between the points $\varphi = \pi/4$ and $3\pi/4$ (Fig. 3) with distances obtained from integration of Eq. (4) we obtain $\chi_a H^2/K_B = 5.2\cdot10^5\,\mathrm{cm}^{-2}$ and $\chi_a H^2/K_S = 1.42\cdot10^5\,\mathrm{cm}^{-2}$. Using these relations, Eq. (4) was integrated across the whole wall, which gave the distribution of the **c**-director in π-walls. The calculated distribution is shown in Fig. 3 by solid and open points. The agreement of our calculations with experiment is clearly good. A similar procedure was used to calculate the orientation of the **c**-director across the 2π-wall. Comparing the distances in the 2π-wall between the points $\varphi = \pi/4$ and $7\pi/4$, between $\varphi = 3\pi/4$ and $5\pi/4$ with the distances obtained from integration of Eq. (5), the ratios $PE/K_S = 1.65\cdot10^5\,\mathrm{cm}^{-2}$ and $PE/K_B = 4.95\cdot10^5\,\mathrm{cm}^{-2}$ were obtained. Using these ratios Eq. (5) was integrated over the wall. The calculated orientation of the **c**-director across the 2π-wall is shown in Fig. 4 by closed points. Using the obtained values of the ratios PE/K_S, PE/K_B and $E = 11.5\,\mathrm{V/cm}$, $P = 3.84\,\mathrm{nC/cm}^2$, the bend and splay elastic constants are determined: $K_S = 2.67\cdot10^{-6}\,\mathrm{erg/cm}$ and $K_B = 0.89\cdot10^{-6}\,\mathrm{erg/cm}$. We performed measurements of the wall structure in the temperature range from 104 °C to 79 °C. In this range the ratio of the elastic constants K_B/K_S does not depend on temperature with an accuracy of ±10 percent. This correlates with behavior of the bulk sample in which the tilt angle practically does not depend on temperature. The ratio K_B/K_S correlates with results of previous measurements [8–9, 17–21]. We may conclude that the structure of the walls is well described by the theory with anisotropic elasticity of the **c**-director field.

In conclusion, we measured for the first time the structure of π-walls and 2π-walls in smectic films, that is the distribution of the **c**-director orientation across the walls. Our studies allow to analyze the structure of π-walls and 2π-walls in detail. The **c**-director orientation across the walls cannot be described by theory in the one-constant approximation. Our results demonstrate that the π-wall structure essentially depends on the wall orientation with respect to the field. Comparison with theory allows us to understand the observed peculiarities of the wall structure.

This work was supported in part by RFFI Grants # 11-02-01028, 11-02-01424, and 11-02-92610, and by Grant # MK-2458.2011.2. We thank H.T. Nguyen, A. Babeau, and S. Gineste for the synthesis of the liquid crystals.

1. P.G. de Gennes and J. Prost, *The Physics of Liquid Crystals*, 2nd ed., Clarendon Press, Oxford, 1993.
2. P.M. Chaikin and T.C. Lubensky, *Principles of Condensed Matter Physics*, Cambridge University Press, Cambridge, 2000.
3. N. A. Clark and S. T. Lagerwal, Appl. Phys. Lett. **36**, 89 (1980).
4. R. Pindak, C.Y. Young, R.B. Meyer, and N.A. Clark, Phys. Rev. Lett. **45**, 1193 (1980).
5. D.R. Link, J.E. Maclennan, and N. A. Clark, Phys. Rev. Lett. **77**, 2237 (1996).
6. P.V. Dolganov, E.I. Demikhov, Y. Suzuki, and A. Fukuda, JETP **95**, 728 (2002) [ZhETF **122**, 840 (2002)].
7. Y. Galerne and L. Liebert, Phys. Rev. Lett. **64**, 906 (1990).
8. P.V. Dolganov and B.M. Bolotin, Pis'ma v ZhETF **77**, 503 (2003) [JETP Lett. **77**, 429 (2003)].
9. P.V. Dolganov, B.M. Bolotin, and A. Fukuda, Phys. Rev. E **70**, 041708 (2004).
10. P. Pieranski, L. Bieliard, J.-Ph. Tournelles et al., Physica A **194**, 364 (1993).
11. P. Cluzeau, M. Ismaili, A. Annakar et al., Mol. Cryst. Liq. Cryst. **362**, 185 (2001).
12. P.V. Dolganov, E.I. Kats, V.K. Dolganov, and P. Cluzeau, Pis'ma v ZhETF **90**, 424 (2009) [JETP Lett. **90**, 382 (2009)].
13. M.-H. Lu, K. A. Crandall, and C. Rosenblatt, Phys. Rev. Lett. **68**, 3575 (1992).
14. T. Stoebe, P. Mach, and C. C. Huang, Phys. Rev. Lett. **73**, 1384 (1994).
15. M. Born and E. Wolf, *Principles of Optics*, Pergamon, New York, 1964.
16. R. Stannarius, J. Li, and W. Weissflog, Phys. Rev. Lett. **90**, 025502 (2003).
17. J.-B. Lee, R. A. Pelcovits, and R.B. Meyer, Phys. Rev. E **75**, 051701 (2007).
18. Y. Galerne and R. Najjar, Phys. Rev. E **69**, 031706 (2004).
19. D.R. Link, N. Chattham, J.E. Maclennan, and N.A. Clark, Phys. Rev. E **71**, 021704 (2005).
20. A. Eremin, C. Bohley, and R. Stannarius, Eur. Phys. J. E **21**, 57 (2006).
21. A. Eremin, C. Bohley, and R. Stannarius, Phys. Rev. E **74**, 040701(R) (2006).